

Article

Geochemical Behavior of Sedimentary Phosphorus Species in Northernmost Artificial Mangroves in China

Shuzhen You ¹, Peisun Loh ^{1,*}, Zilong Li ¹, Haiyan Qin ², Siriporn Pradit ³, Thi Phuong Quynh Le ⁴,
Chantha Oeurng ⁵, Che Abdul Rahim Mohamed ⁶, Choon Weng Lee ⁷, Xixi Lu ⁸, Gusti Z. Anshari ⁹,
Selvaraj Kandasamy ¹⁰, Jianjun Wang ^{11,12}, Lili Ji ¹³ and Jian Guo ¹⁴

- ¹ Institute of Marine Geology and Resources, Ocean College, Zhejiang University, Zhoushan 316021, China; yousz@zju.edu.cn (S.Y.); zilongli@zju.edu.cn (Z.L.)
 - ² The 11th Geological Section of Zhejiang Province, Wenzhou 325006, China; haiyanqin.geo@gmail.com
 - ³ Coastal Oceanography and Climate Change Research Center, Faculty of Environmental Management, Prince of Songkla University, Songkhla 90110, Thailand; siriporn.pra@psu.ac.th
 - ⁴ Institute of Natural Product Chemistry, Vietnam Academy of Science and Technology, Hanoi 11307, Vietnam; quynhlt@gmail.com
 - ⁵ Faculty of Hydrology and Water Resources Engineering, Institute of Technology of Cambodia, Phnom Penh 12156, Cambodia; chantha@itc.edu.kh
 - ⁶ Faculty of Science and Technology, Universiti Kebangsaan Malaysia, Bangi 43600, Malaysia; carmohd@ukm.edu.my
 - ⁷ Institute of Biological Sciences, Universiti Malaya, Kuala Lumpur 50603, Malaysia; lee@um.edu.my
 - ⁸ Department of Geography, National University of Singapore, 10 Kent Ridge Crescent, Singapore 119260, Singapore; geoluxx@nus.edu.sg
 - ⁹ Soil Science Department, Faculty of Agriculture, Tanjungpura University, Pontianak 78124, Indonesia; gzanshari@live.untan.ac.id
 - ¹⁰ Department of Geological Oceanography, Xiang'an Campus, Xiamen University, Xiamen 361102, China; selvaraj@xmu.edu.cn
 - ¹¹ Jiangsu Key Laboratory of Crop Genetics and Physiology/Jiangsu Key Laboratory of Crop Cultivation and Physiology, Agricultural College of Yangzhou University, Yangzhou 225009, China; wangjianjun@yzu.edu.cn
 - ¹² Jiangsu Co-Innovation Centre for Modern Production Technology of Grain Crops, Yangzhou University, Yangzhou 225009, China
 - ¹³ Institute of Innovation and Application, Zhejiang Ocean University, Zhoushan 316022, China; jilili@zjou.edu.cn
 - ¹⁴ Zhoushan Sailaite Ocean Technology Co., Ltd., Zhoushan 316100, China; jguo.co@gmail.com
- * Correspondence: psloh@zju.edu.cn



Citation: You, S.; Loh, P.; Li, Z.; Qin, H.; Pradit, S.; Le, T.P.Q.; Oeurng, C.; Mohamed, C.A.R.; Lee, C.W.; Lu, X.; et al. Geochemical Behavior of Sedimentary Phosphorus Species in Northernmost Artificial Mangroves in China. *Forests* **2022**, *13*, 610. <https://doi.org/10.3390/f13040610>

Academic Editors: Victor H. Rivera-Monroy, Xosé Lois Otero-Pérez, Jorge Lopez-Portillo and Tiago Osorio Ferreira

Received: 18 February 2022

Accepted: 11 April 2022

Published: 14 April 2022

Publisher's Note: MDPI stays neutral with regard to jurisdictional claims in published maps and institutional affiliations.



Copyright: © 2022 by the authors. Licensee MDPI, Basel, Switzerland. This article is an open access article distributed under the terms and conditions of the Creative Commons Attribution (CC BY) license (<https://creativecommons.org/licenses/by/4.0/>).

Abstract: Mangroves are typically found in tropical coastal areas, and these ecosystems face deterioration and loss due to threats from climate and human factors. In this study, sediment cores were collected from human-planted mangroves in sub-tropical Ximen Island, China, and were determined for sedimentary phosphorus (P) species. The objective was to investigate the ability of mangroves planted in a zone bordering their temperature limit to preserve and regulate P. Our results showed that bioavailable P (BAP), which includes exchangeable-P (Ex-P), iron-bound P (Fe-P), and organic P (OP), accounted for approximately 64% of total P (TP). Apatite P (Ca-P), which accounted for 24% of TP, most likely originated from aquaculture activities surrounding the island. The vertical distribution of sedimentary P species along the sediment cores showed a rather constant trend along the salt marsh stand but considerable fluctuations for the mangroves and bare mudflat. These results indicate that mangroves accumulated P when there was a high P discharge event, and that this P was eventually released during organic matter decomposition and contributed to Ca-P formation. Nevertheless, old and young mangroves accumulated higher sedimentary P species, OP, and BAP compared to the salt marsh stand and bare mudflat areas. This study showed the potential of mangroves planted outside their suitable climate zone to preserve and regulate P.

Keywords: human perturbations; sedimentary P dynamics; artificial subtropical mangrove; wetland ecosystems; Ximen Island

1. Introduction

Mangroves are intertidal ecosystems typically found in shallow-area transition zones from land to sea. Mangrove forests are important blue carbon ecosystems that not only serve as carbon reservoirs [1–3], but also provide ecosystem services by regulating organic pollutants, heavy metals [4–6], nutrients [7–9], and microplastics [10,11] along coastal zones. In addition, these ecosystems are habitats for many animals [9,12] and provide important means of livelihood, such as fishing [13,14] and tourism industries [15,16]. However, mangrove forests are seriously threatened by climate change factors, such as sea level rise [17,18]; human activities, such as land use and deforestation [19,20]; pollution [21,22]; and debris problems [23]. Realizing the fact that mangroves are facing serious degradation and loss has prompted various restoration efforts, such as hydrological and community-based ecological restoration and sowing of seedlings and propagules [24,25]. These restoration and conservation efforts have enhanced the tree density and maintained species diversity in mangrove ecosystems [26,27]. Mangrove forests took only five years after restoration to obtain their maximum protection capacity [28]. In addition, the values of carbon sequestration, ecotourism, and forest and fishery products exceeded the cost of rehabilitation [27,29], supporting the importance of restoration, rehabilitation, and conservation works on mangrove forests.

The content, form, and distribution of biogenic elements in sediments are influenced by atmospheric deposition, terrestrial input, and human activities [30,31], and sediments provide records of these past events. The enrichment and release of phosphorus (P) in mangroves is a key factor leading to eutrophication in coastal waters. Meanwhile, an increasing awareness of environmental protection has somewhat reduced the input of P from external sources; however, the problems related to P pollution remain serious. Studies of different sedimentary P species in lake sediments have demonstrated the occurrence of P release from sediments [32,33]. In addition, a few P species, such as the exchangeable-P (Ex-P), iron-bound P (Fe-P), and organic P (OP), can be released from sediments into overlying water and become bioavailable [34,35]. Therefore, the understanding of the dynamics of sedimentary P species needs to be improved. Although sedimentary P species have been extensively studied in lakes and coastal areas [36–41], only a few studies have been conducted on mangrove systems [42,43], especially on human-planted mangroves in a sub-tropical zone.

The natural distribution of Chinese mangroves is from Yulin Harbour (18°09' N) in Hainan Province to Fuding (27°20' N) in Fujian Province, and the northernmost limit of artificial mangroves is Ximen Island (28°21' N), Wenzhou, Zhejiang Province [44,45]. The mangrove ecosystem of Ximen Island is currently the northernmost artificial mangrove in China that can self-reproduce. The mangrove was introduced from Fujian in 1957 and planted with *Kandelia obovata*. Previous studies on the mangroves in Ximen Island involved the determination of microbial distribution and environmental characteristics of mangrove sediments [46,47], investigation of the annual growth of different mangrove species in experimental plots [48,49], and studying the ecological relation between the benthic community and mangrove forest [50,51]. However, little is known about the feasibility of these northernmost human-planted mangrove systems to regulate P. For this purpose, sediment cores were collected from two mangrove systems on Ximen Island: younger (approximately 4 years old) and older (approximately 60 years old) mangrove forests. To our knowledge, this is the first study conducted to determine the sedimentary P species in the northernmost human-planted mangroves in China. This study aimed to determine how well artificial mangroves situated in the coldest temperature limit to their growth fare in preserving and regulating P in their sediments. The study results will provide important information to policy makers on the potential of mangrove planting.

2. Materials and Methods

2.1. Study Area and Sampling Locations

Ximen Island is located off Wenzhou, Zhejiang Province, China. It is the largest island in the northern part of Yueqing Bay, Zhejiang Province, with a land area of 6.97 km², a beach

area of 19.20 km², and a coastline length of 11.81 km [44,52]. The low-temperature-resistant mangrove plant *Kandelia obovata* was introduced from Fujian into Ximen Island in 1957, and since then, the mangrove area has reached approximately 0.33 km² through natural breeding [53,54]. The island has a subtropical monsoon climate, with an average annual temperature of 17–18 °C and an average annual precipitation of 1700 mm. The tides in Yueqing Bay showed irregular and semi-diurnal variation, with an average variation of 4.2 m and a maximum variation of 8.34 m [44,47]. The mangrove wetland of Ximen Island is rich in biodiversity and there are no streams on the island [48,52].

Four sediment cores were successfully collected from Ximen Island mangroves on 28 and 29 May 2021. The cores were collected from two mangrove areas (M1 and M2), where M1 was the older mangrove system of approximately 60 years old and M2 was the younger mangrove system of approximately 4 years old. Two locations were sampled in each mangrove area. In M1, L1 was located on the landward side and had mangrove vegetation, and S1 was located at the fringe of the mangrove coastal area and had salt marsh plants *Spartina alterniflora*. In M2, L2 was the landward location with younger mangrove plants, and S2 was a bare mudflat near the coastal area (Table 1; Figure 1). Sediment cores were collected using a peat auger with a length of 1 m and an inner diameter of 6 cm. The cores were of lengths 100 cm (L1, S1, and L2) and 96 cm (S2). At each location, three cores were collected, and samples of sediment slices at 2-cm intervals were pooled from the three cores and then immediately placed in an incubator. The sediments were dried at approximately 45 °C for three days in the laboratory. Debris, such as dead branches and leaves, were removed. The sediments were then ground with a mortar and pestle until homogenous and ready for subsequent analyses.

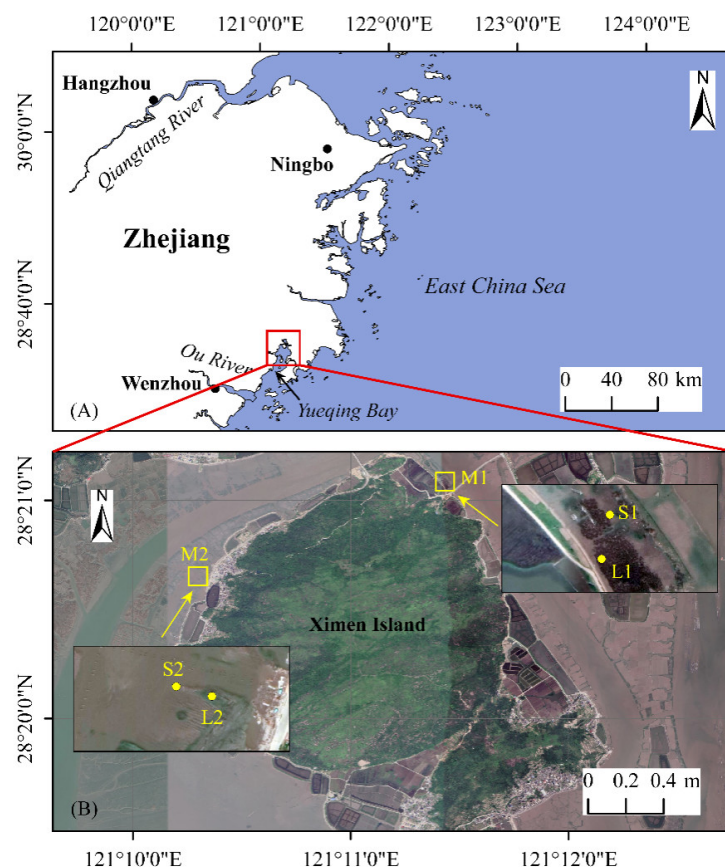


Figure 1. (A) Map showing the Ximen Island mangrove area in the northern part of Yueqing Bay, Zhejiang Province; (B) magnification of the four sampling locations (L1, S1, L2, S2) from two mangrove ecosystems (M1 and M2) are set in the mangrove area.

Table 1. Sampling locations and samples information.

Sampling Sites	Locations		Core Length (cm)	Number of Samples	Other Information
	Latitude	Longitude			
M1-L1	28°21′05″ N	121°11′26″ E	100	26	Covered by an old mangrove forest and with the effects from the cold.
M1-S1	28°21′04″ N	121°11′25″ E	100	26	In the seaward vegetation transition zone which has <i>Spartina alterniflora</i> .
M2-L2	28°20′39″ N	121°10′19″ E	100	26	Covered by young <i>Kandelia obovata</i> plant.
M2-S2	28°20′39″ N	121°10′18″ E	96	25	In mudflat on the seaward side.

2.2. Sequential P Extraction

Different sedimentary P species were extracted using Ruttenberg's (1992) sequential extraction method [55,56]. In the first step, 0.3 g of dry sediment was weighed into a 50-mL centrifuge tube, to which 20 mL of 1 M MgCl₂ was added, and the solution pH was adjusted to 8 with 10 M NaOH solution. Extraction was performed by shaking the solution for 2 h at room temperature (RT), after which the content was centrifuged and the supernatant was decanted and set aside. Another 20 mL of 1 M MgCl₂ was added to the residue, and the process was repeated. The residue was washed with 10 mL of H₂O for 2 h and centrifuged. All supernatants were saved to determine their Ex-P content. In the second step, 20 mL of citrate–dithionite–bicarbonate solution (32.4 g C₆H₅Na₃O₇ · 2H₂O + 42 g NaHCO₃ + 2.87 g Na₂S₂O₄ in 500 mL distilled water) was added to the residue, and the solution was shaken for 8 h at RT. The content was centrifuged, and the supernatant was decanted and saved. Then, 20 mL of 1 M MgCl₂ was added to the residue and shaken for 2 h, followed by centrifugation and supernatant extraction. Subsequently, the residue was washed with 10 mL of H₂O for 2 h, centrifuged, and then all of the supernatant was removed and saved for Fe-P determination. For the next fraction, 20 mL of 0.2 M acetate buffer (pH = 4) was added to the remaining residue and shaken for 6 h at RT, after which the mixture was centrifuged and the supernatant was saved. The residue was then washed twice with 1 M MgCl₂, centrifuged again, and the supernatant was removed and set aside. The residue was finally washed with 10 mL of H₂O, centrifuged once more, and the supernatant was removed and saved. The supernatants obtained from this step were determined for authigenic P (Ca-P) content. In the next step, 1 M HCl was added to the residue and shaken for 16 h, after which the content was centrifuged, and the supernatant was saved for the analysis of detrital apatite P (De-P). The residue was then moved to a crucible and dried in an oven at 80 °C for one day, followed by combustion at 550 °C for 5 h. The residue was cooled, added with 1 M HCl, and shaken for 16 h, and the supernatant was determined for OP content. All P concentrations were determined colorimetrically as molybdenum blue complexes using a UV-visible spectrophotometer UV-8000 (METASH, Shanghai, China). Absorbance was measured at a wavelength of 885 nm. Inorganic P (IP) is the sum of Ex-P, Fe-P, Ca-P, and De-P; total P (TP) is the sum of all P fractions (or the sum of IP and OP); and bioavailable P (BAP) is the sum of Ex-P, Fe-P, and OP.

2.3. Statistics and Visualization

Pearson correlation analysis and two-tailed significance tests were conducted to determine the correlation between the different parameters. Correlations were considered significant at $p < 0.05$. Data analyses were conducted using IBM SPSS for Windows (Version 26.0, Armonk, NY, USA), and the “±” symbol represents the standard deviation. The maps and diagrams were mainly produced using Origin (Version 2018, Northampton, MA, USA).

3. Results

The results of sedimentary P forms and percentages of OP, IP, and BAP to TP are presented in Appendix A. Table 2 shows the ranges and mean values of the different sedimentary P species and TP. The ranges of TP concentrations for the old mangrove (L1), salt marsh (S1), young mangrove (L2), and bare mudflat (S2) were 79.45–113.99, 63.91–89.90, 77.24–125.34, and 44.58–84.36 mg/kg, respectively. The young mangrove had the highest mean TP (97.95 mg/kg), followed by the old mangrove (TP = 93.16 mg/kg), zone

with salt marsh plants *S. alterniflora* (TP = 75.84 mg/kg), and bare mudflat (TP = 67.53 mg/kg). The old mangrove and *S. alterniflora* stand accumulated the highest Ex-P and Fe-P concentrations, followed by the young mangrove and mudflat; the old and young mangroves accumulated higher Ca-P, IP, OP, and BAP concentrations than salt marsh and mudflat. Overall, the old and young mangroves accumulated higher P in their sediments than salt marshes and mudflats.

Table 2. Ranges and mean, and percentage ranges and mean, of each sediment P to TP.

	M1-L1	M1-S1	M2-L2	M2-S2	All
Ex-P (mg/kg)	28.01–49.21	30.24–46.31	31.67–46.23	27.95–41.82	27.95–49.21
Mean	39.19	38.66	36.30	32.83	36.75
Ex-P/TP	29.30–49.92%	38.10–58.22%	28.95–47.21%	39.34–69.34%	29.30–69.34%
Mean	42.06%	50.98%	37.05%	48.61%	44.68%
Fe-P (mg/kg)	0.46–15.80	2.33–9.68	2.30–8.13	0.49–16.30	0.46–16.30
Mean	4.85	5.86	3.84	4.30	4.71
Fe-P/TP	0.51–15.49%	3.05–12.09%	2.20–8.04%	0.73–21.66%	0.51–21.66%
Mean	5.21%	7.73%	3.92%	6.37%	5.81%
Ca-P (mg/kg)	20.68–41.53	12.29–36.16	12.71–56.27	1.89–17.42	1.89–56.27
Mean	27.80	18.57	29.65	7.18	20.80
Ca-P/TP	22.76–45.82%	18.66–45.56%	12.82–46.02%	2.64–23.85%	2.64–45.82%
Mean	29.84%	24.48%	30.27%	10.63%	23.81%
De-P (mg/kg)	1.49–14.67	2.64–10.47	4.95–31.57	1.89–26.29	1.49–31.57
Mean	6.05	5.24	15.62	14.63	10.39
De-P/TP	1.64–15.35%	2.94–16.10%	5.45–30.93%	3.73–32.64%	1.64–21.64%
Mean	6.49%	6.90%	15.95%	21.66%	12.75%
OP (mg/kg)	7.50–21.56	3.23–17.97	3.91–25.14	1.95–24.58	1.95–25.14
Mean	15.28	7.51	12.55	8.96	11.08
OP/TP	8.13–23.35%	4.84–19.99%	4.24–27.64%	4.37–33.76%	4.24–33.76%
Mean	16.46%	9.65%	12.73%	13.15%	13.00%
IP (mg/kg)	66.83–97.68	58.85–75.65	63.94–111.31	42.56–79.49	42.56–111.31
Mean	77.89	68.33	85.41	58.58	72.55
IP/TP	76.65–91.87%	80.01–95.16%	72.36–95.76%	66.24–95.63%	66.24–95.76%
Mean	83.54%	90.35%	87.27%	86.85%	87.00%
BAP (mg/kg)	43.25–80.39	40.19–62.53	42.11–70.51	34.19–62.52	34.19–80.39
Mean	59.32	52.04	52.69	45.73	52.45
BAP/TP	47.72–71.30%	50.99–74.51%	43.19–77.51%	57.48–85.86%	43.19–85.86%
Mean	63.64%	68.71%	54.20%	68.22%	63.69%
TP (mg/kg)	79.45–113.99	63.91–89.90	77.24–125.34	44.58–84.36	44.58–113.99
Mean	93.16	75.84	97.95	67.53	83.62

Based on the ranges of concentrations of different sedimentary P species along the four cores in both mangroves, the contribution of each P form to TP were in the following order: Ex-P > Ca-P > OP > De-P > Fe-P. The order of the different P species varied slightly for each location: L1 (Ex-P > Ca-P > OP > De-P > Fe-P), S1 (Ex-P > Ca-P > OP > Fe-P > De-P), L2 (Ex-P > Ca-P > De-P > OP > Fe-P), S2 (Ex-P > De-P > OP > Ca-P > Fe-P). The order of BAP concentrations for the four locations was as follows: L1 > L2 > S1 > S2 (Table 2). Comparison of the sedimentary P species in the surface sediment at different locations also showed a similar order as the overall ranges of different sedimentary P species and BAP, as follows: L1 > L2 > S1 > S2 (Figure 2).

Fe-P, De-P, and OP showed a general trend of decrease from 100 cm to the surface sediment along L1, L2, and S2 cores. These P species showed a rather constant trend along S1, except for the highest OP observed at 4–12 cm. Ex-P along L1 decreased from 100 cm to approximately 74–76 cm and then started to increase toward the 22–24 cm layer, followed by decreasing trend toward the surface sediments. Ex-P along S1 remained constant from 100 to 20 cm and then decreased from approximately 20 cm toward the surface sediments. Ex-P along the M2 cores (L2 and S2) showed a decrease from 100 cm to the surface sediments. In contrast, Ca-P along the M1 (L1 and S1) and S2 cores showed an increasing trend toward the surface sediment, while Ca-P along L2 showed an overall decreasing trend toward the surface sediments, except for a drastic increase at approximately 30 cm. Both IP and TP exhibited the same trend; they were relatively lower before 30 cm, showed the highest value at approximately 30 cm, and then a decreasing trend from approximately 30 cm toward the surface sediments, except for the salt marsh, which showed a gradual increase in IP and TP from approximately 30 cm toward the surface sediments

(Figure 3). The BAP concentration was rather constant along L1 below the 40 cm layers, showed the highest concentrations at approximately 25–40 cm, and then decreased toward the surface sediments. The BAP concentration remained constant throughout S1, except for the drastic decrease in the surface sediment. It exhibited a decreasing trend from the bottom to the surface layer of L2 and showed a decreasing trend from 36 cm toward the surface sediment along the core S2 (Figure 4).

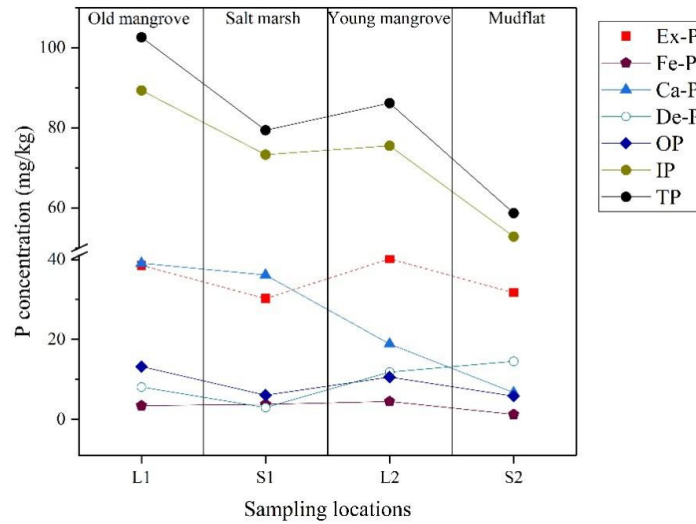


Figure 2. P species in the surface sediments (0–2 cm) of the Ximen Island mangrove ecosystems.

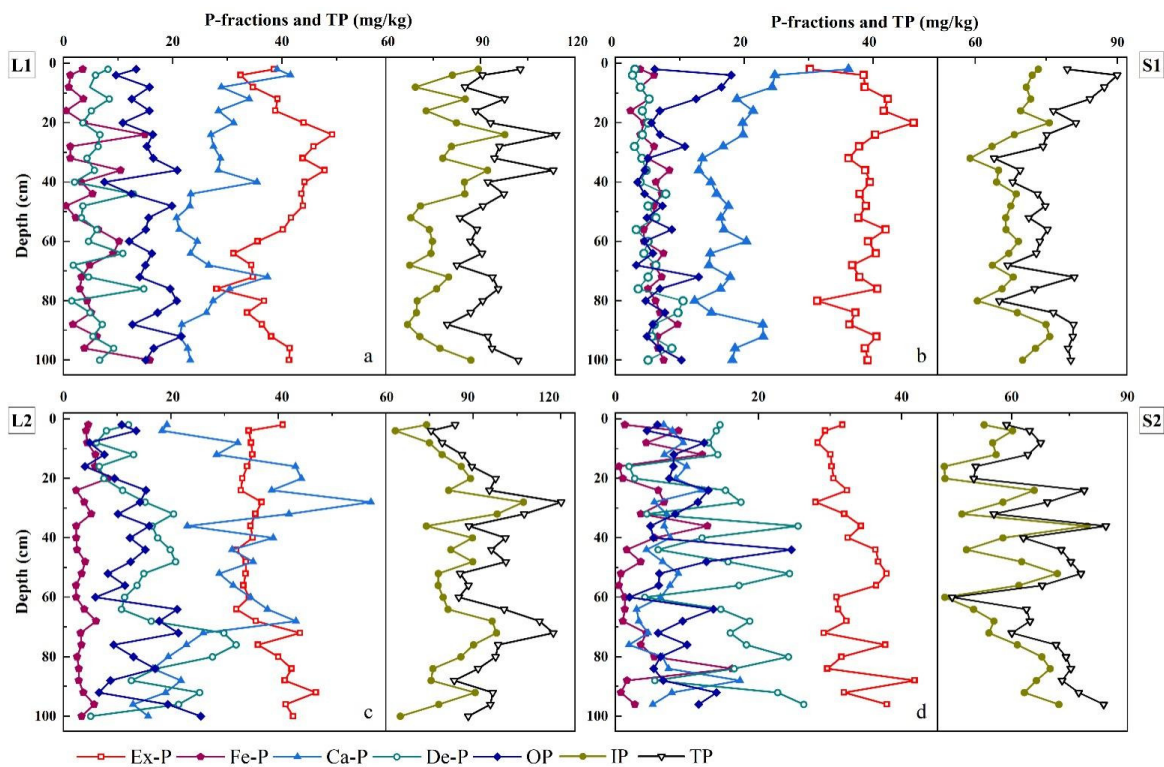


Figure 3. Trends of the Ex-P, Fe-P, Ca-P, De-P and OP concentrations (pictured left of each plot) and details of IP and TP fractions (pictured right of the plots) along the sediment cores. The X-axes represent the concentrations of the sedimentary P species, labels on the Y-axis indicate the depths of the sediment cores.

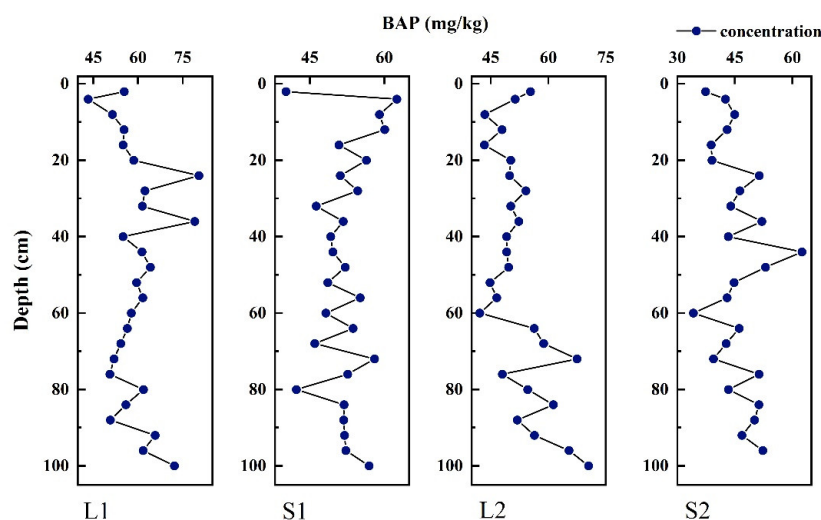


Figure 4. The vertical variations of BAP fractions (Ex-P, Fe-P, and OP) along the sediment cores.

4. Discussion

4.1. Sedimentary P Species

Different sedimentary P species can indicate the sources and bioavailability of P in the sediment. For instance, Ex-P has been related to wastewater discharge [39,57], and sewage and shrimp farms have affected mangroves [21,42]. Fe-P is also an indicator of anthropogenic pollution. A low Fe-P concentration is usually associated with oxygen depletion, as Fe-P can be released from sediments in reducing environments; high pH and bacterial activity also enhances the release of Fe-P [58–60]. OP can originate from wastewater and mariculture activities [39,61] and can be released by mineralization and become bioavailable [61,62]. In contrast, De-P is an inert and stable fraction that usually originates from land sources such as rivers [39,63]. The Ca-P sources include carbonate-associated P; biogenic apatite, such as bones and teeth; and authigenic fluorapatite [39,64,65]. The mineralization of organic matter can release phosphate, which is then adsorbed by clay minerals and the surface of Fe oxides. Some of the OP released upon organic matter decomposition and the P released from the Fe-P fraction result in the formation and accumulation of Ca-P in sediments [62,63,66,67].

The sediment cores from the mangroves on Ximen Island exhibited the highest proportion of Ex-P, which accounted for an average of 45% of TP. The proportion of OP accounted for 13% of TP, and that of Fe-P accounted for 5.81% of TP in the mangroves on Ximen Island. We presume that wastewater from household and farming activities along the coastal areas surrounding the island could be the main contributor to the high Ex-P, Fe-P, and OP proportions in these mangroves. The second highest Ca-P species, which accounted for a mean of approximately 24% of TP, was likely attributed to the aquaculture activities conducted along the coastal zones surrounding the island. Shrimp farm-impacted mangroves usually have a high Ca-P content due to fertilization with inorganic phosphate and liming at shrimp ponds [34,42,68]. The low Fe-P content in these mangroves is attributable to the release of some of this P from sediments under anoxic conditions after a period of prolonged inundation. As the rivers discharged from the mainland surrounding Yueqing Bay contribute fewer materials to the bay compared to the contributions from the Changjiang River [69,70], the low De-P concentration in these mangrove systems (12.75% of TP) indicates a lesser contribution of P from the adjacent rivers.

Comparison with the sedimentary TP contents in other mangroves such as the Jiulong estuary mangrove (TP = 821–1689 mg/kg; Jiang et al., 2018) and Quanzhou Bay mangrove (TP = 492–726 mg/kg; Le et al., 2022) in China, and the surface sediment (TP = 451–552 mg/kg) and sediment cores (TP = 459–530 mg/kg) of the Pichavaram mangrove in India [71], shows that the mangroves in Ximen Island have a relatively low TP (44.58–113.99 mg/kg; Table 3). Similar to Jiulong estuary and Quanzhou Bay mangroves, the mangroves in Ximen Island showed high contents of BAP, thus indicating that these mangroves have a potential to release BAP to the coastal water. The surface sedimentary P

species of the Pichavaram mangroves are in this order: Fe-P > Ca-P > De-P > OP > Ex-P. Thus, the sediments of the Pichavaram mangroves could be releasing P under anoxic conditions whilst the sediments of the Ximen Island mangroves could be releasing P under normal perturbations and during organic matter decomposition.

Table 3. Comparison of the concentrations of sedimentary P species in the present study with those in other mangrove areas reported in the literature.

Study Area	Concentrations (mg/kg)							References
	Ex-P	Fe-P	Ca-P	De-P	OP	IP	TP	
The Jiulong Estuary mangrove, China	-	223–793	-	100–200	100–200	721–1489	821–1689	Jiang et al., 2018 [43]
Surface sediments in the Pichavaram mangrove, India	49.6	172	122	92	58	403–473	451–552	Prasad and Ramanathan, 2010 [71]
Core sediments in the Pichavaram mangrove, India	29	126	144	138	450	-	459–530	Prasad and Ramanathan, 2010 [71]
The Ximen Island mangrove, China	36.75	4.71	20.80	10.39	11.08	42.56–111.31	44.58–113.99	This study
	HCl-P	NaOH-P	-	BAP	OP	IP	TP	
Quanzhou Bay mangrove wetland, China	60–96	107–151	-	63–106	144–192	297–530	492–726	Le et al., 2022 [72]

4.2. Different Wetland Ecosystems

The accumulation of mangrove plants, litterfall, root, algae, seagrass, and phytoplankton materials can enhance soil carbon, nutrients, and OP in mangrove sediments [43,73]. L1 and L2 exhibited higher contents of sedimentary P species, as well as IP, BAP, and TP, followed by S1 and S2, indicating that mangroves can accumulate P better than the salt marsh stand and bare mudflat. Other studies have also demonstrated that the *Spartina alterniflora* stand has a lower TP content than the natural *Kandelia obovata* mangrove forest, indicating the effectiveness of mangrove sediments to trap nutrients. Accordingly, the low BAP concentration in *Spartina alterniflora* sediments was attributed to the transfer of P from the sediment to the tissues of *Spartina alterniflora* for their growth [74,75]. The lowest BAP and TP concentrations, as well as most of the P species in S2, further proves that non-vegetated wetland ecosystems are less efficient in trapping nutrients than vegetated wetland ecosystems. Mangrove forests have been found to be able to remove nutrients from tidal water [8,76]. Besides, nutrients produced during mangrove litter decomposition can be re-absorbed by mangrove forests [73,77]. Thus, the efficiency of mangrove to trap nutrients results in increased P content with mangrove restoration [74].

4.3. Vertical Distribution of Sedimentary P Species

Some studies have shown a trend of decreasing P with increasing depth due to the degradation process over time and the loss of sedimentary P to the overlying water column [78,79]. Other studies have also shown that a period of stronger P enrichment can reflect the influence of human activities and untreated sewage [39,61,79]. The sedimentary P species, IP, and TP along the cores of both mangrove systems in Ximen Island showed considerable fluctuations. The trends of OP and Ex-P were quite similar to that of BAP (based on significant correlation results, $p < 0.01$; Table 4), all showing a decreasing trend, followed by an increasing trend and then an overall decreasing trend from the core bottom toward the present. These mangroves most probably received P from the various activities conducted in the surrounding areas, such as farming, mariculture, and household waste. In addition, they were subjected to replanting and pesticide pollution. Unlike the rather constant BAP in the salt marsh stand, which indicated a steady absorption of P by *S. alterniflora* plants, the sudden increases in the sedimentary P species and BAP, IP, and TP at the mangrove locations indicate the potential of mangrove systems to accumulate P under the occurrences of high P discharge events. Peak sedimentary P species are usually followed by decreasing trends, indicating the occurrence

of the processes of organic matter decomposition and absorption of P by mangrove plants. Studies have found that variations of the concentrations of Ex-P, Fe-P, Ca-P and OP could be due to transformation of these sedimentary P species during burial [73]. In the Ximen Island mangrove, some of the bioavailable P released from the sediments are then transformed into Ca-P. Thus, a simultaneous increasing trend in Ca-P (significant negative correlation with BAP, $p < 0.05$; Table 4) further demonstrated that besides the contribution from shrimp farming activities, some of this Ca-P is attributable to the release of the BAP fraction. Mangrove systems usually show stronger P deposition in summer and autumn due to the enhanced inputs of labile organic matter. The sediments then release P into the overlying water [35], especially during the flood season in the subsequent spring and summer, when oxygen depletion most likely occurs and the microbial iron reduction process is predominant within the top layer of the sediment [59,80].

Table 4. Pearson’s correlations between phosphorus fractions from the sediment cores of Ximen Island mangrove.

	Ex-P	Fe-P	Ca-P	De-P	OP	IP	BAP	TP
(a) M1-L1 ($n = 26$)								
Ex-P	1							
Fe-P	0.218	1						
Ca-P	−0.160	−0.280	1					
De-P	−0.232	0.132	−0.060	1				
OP	−0.014	0.127	−0.457 *	0.055	1			
IP	0.550 **	0.496 *	0.429 *	0.260	−0.242	1		
BAP	0.737 **	0.685 **	−0.430 *	−0.059	0.468 *	0.494 *	1	
TP	0.552 **	0.556 **	0.241	0.288	0.180	0.911 **	0.700 **	1
(b) M1-S1 ($n = 26$)								
Ex-P	1							
Fe-P	−0.195	1						
Ca-P	−0.187	−0.35	1					
De-P	−0.286	0.378	−0.388	1				
OP	0.128	−0.131	0.322	−0.348	1			
IP	0.311	0.004	0.696 **	−0.047	0.25	1		
BAP	0.646 **	0.095	0.015	−0.315	0.778 **	0.377	1	
TP	0.284	−0.075	0.657 **	−0.238	0.760 **	0.819 **	0.713 **	1
(c) M2-L2 ($n = 26$)								
Ex-P	1							
Fe-P	−0.097	1						
Ca-P	−0.596 **	0.273	1					
De-P	0.375	−0.265	−0.239	1				
OP	0.233	−0.169	−0.209	0.11	1			
IP	0.007	0.197	0.649 **	0.513 **	−0.072	1		
BAP	0.702 **	0.025	−0.426 *	0.233	0.828 **	−0.009	1	
TP	0.111	0.106	0.507 **	0.525 **	0.383	0.894 **	0.365	1
(d) M2-S2 ($n = 25$)								
Ex-P	1							
Fe-P	−0.331	1						
Ca-P	0.212	−0.01	1					
De-P	0.157	0.265	−0.31	1				
OP	0.157	−0.249	−0.214	−0.029	1			
IP	0.430 *	0.446 *	0.167	0.805 **	−0.128	1		
BAP	0.515 **	0.222	−0.036	0.254	0.684 **	0.479 *	1	
TP	0.480 *	0.314	0.063	0.754 **	0.325	0.896 **	0.763 **	1

Pearson correlation is used to determine the relationships among the P fractions. Results of correlation coefficient (r) are presented in the table; n = sample size; * indicates p is significant at the 0.05 level, ** indicates p is significant at the 0.01 level, the numbers not marked by * or ** indicate no significant correlation between the two parameters.

5. Conclusions

The dynamics of sedimentary P species in human planted mangrove systems in Ximen Island, China, were investigated in this study. Sediment cores were collected from two locations in the old mangrove system (M1)—the landward side with an old mangrove of 60 years old (L1) and the seaward side with *Spartina alterniflora* marsh plants (S1)—and two locations from the young mangrove system (M2): the landward side with a young mangrove of 4 years old (L2) and the seaward side, which was a bare mudflat (S2). The order of different sedimentary P forms was as follows: Ex-P (44.68% of TP) > Ca-P (23.81% of TP) > OP (13.00% of TP) > De-P (12.75% of TP) > Fe-P (5.81% of TP). The overall high concentrations of BAP, which was composed of Ex-P, OP, and Fe-P, indicated that these mangrove systems received P input from pollution in the

surrounding areas, and that these sediments could release P during organic matter decomposition and under prolonged inundation. The second most abundant Ca-P might have originated from the aquaculture and shrimp farming activities surrounding the island. Some of this Ca-P could have been contributed by the release of sedimentary BAP. The higher sedimentary P content in the mangroves indicates that mangroves preserve P better than the salt marsh stand and bare mudflat. The salt marsh stand showed a constant distribution of sedimentary P species along the core, indicating the continuous absorption of P by the marsh plants. The sediment cores in the old and young mangrove systems showed an increase in sedimentary P contents during periods of high P discharge; this P was eventually released from the sediments during organic matter decomposition, and some contributed to the Ca-P formation.

Author Contributions: Conceptualization, P.L., S.P., T.P.Q.L., C.O., C.A.R.M., C.W.L., X.L., G.Z.A., S.K. and J.W.; formal analysis, S.Y.; investigation, P.L., S.Y., Z.L., H.Q., L.J. and J.G.; resources, P.L.; data curation, P.L. and S.Y.; writing—original draft preparation, S.Y.; writing—review and editing, P.L.; supervision, P.L.; project administration, P.L.; funding acquisition, P.L. All authors have read and agreed to the published version of the manuscript.

Funding: This research was funded by the Asia-Pacific Network for Global Change Research Fund, grant number CRRP2020–06MY-Loh.

Data Availability Statement: All data in this study is presented in the Appendix A.

Acknowledgments: We are grateful to Xiujian Liu for providing technical assistance and thank Jianjie He, Jianxiong Hu, Xueqi Wang and the villagers of Ximen Island for the assistance provided during our sampling work.

Conflicts of Interest: The authors declare no conflict of interest. Jian Guo, from Zhoushan Sailaite Ocean Technology Co. Ltd, who is responsible for data investigation, does not have any conflict of interest with other authors.

Appendix A

Concentrations of phosphorus species and percentages of OP, IP, and BAP to TP of the four sediment cores in the mangrove area of Ximen Island.

Table A1. Sampling site M1-L1.

Sample Number	Depth (cm)	Ex-P	Concentrations (mg/kg)						TP	Percentage to TP (%)		
			Fe-P	Ca-P	De-P	OP	IP	BAP		OP	IP	BAP
1	0–2	38.56	3.50	39.09	8.15	13.27	89.31	55.34	102.58	12.90%	87.10%	54.00%
2	2–4	32.42	1.23	41.53	5.85	9.60	81.03	43.25	90.63	10.59%	89.41%	47.72%
3	6–8	34.69	0.97	28.90	4.82	15.73	69.38	51.39	85.10	18.48%	81.52%	60.39%
4	10–12	39.19	3.64	33.98	8.35	12.49	85.16	55.32	97.65	12.76%	87.24%	56.68%
5	14–16	38.79	0.46	28.39	5.07	15.73	72.72	54.99	88.45	17.79%	82.21%	62.17%
6	18–20	43.93	3.78	31.13	3.53	10.84	82.37	58.55	93.21	11.63%	88.37%	62.82%
7	22–24	49.21	14.87	26.96	6.64	16.31	97.68	80.39	113.99	14.31%	85.69%	70.52%
8	26–28	45.81	1.22	27.45	6.32	15.25	80.79	62.28	96.05	15.88%	84.12%	64.84%
9	30–32	43.79	1.22	28.73	4.28	16.40	78.02	61.42	94.43	17.37%	82.63%	65.04%
10	34–36	47.78	10.44	28.35	5.63	20.83	92.21	79.06	113.04	18.43%	81.57%	69.94%
11	38–40	44.17	3.27	35.43	1.99	7.50	84.85	54.94	92.35	8.13%	91.87%	59.49%
12	42–44	43.55	5.34	23.31	12.79	12.43	84.99	61.32	97.42	12.76%	87.24%	62.94%
13	46–48	43.82	0.46	23.14	3.52	19.86	70.94	64.13	90.79	21.87%	78.13%	70.63%
14	50–52	41.67	2.25	20.68	3.28	15.59	67.89	59.51	83.48	18.68%	81.32%	71.30%
15	54–56	40.19	6.34	21.18	6.09	15.07	73.80	61.60	88.87	16.96%	83.04%	69.31%
16	58–60	35.53	10.19	24.52	4.56	12.00	74.79	57.72	86.79	13.83%	86.17%	66.50%
17	62–64	31.13	9.07	23.25	10.84	16.19	74.29	56.38	90.48	17.89%	82.11%	62.32%
18	66–68	34.40	4.82	26.59	1.74	14.96	67.55	54.18	82.51	18.13%	81.87%	65.66%
19	70–72	34.70	3.28	37.36	4.56	13.94	79.91	51.92	93.85	14.85%	85.15%	55.33%
20	74–76	28.01	2.99	30.41	14.67	19.52	76.08	50.52	95.60	20.42%	79.58%	52.85%
21	78–80	36.76	4.31	27.38	1.49	20.74	69.93	61.80	90.67	22.87%	77.13%	68.17%
22	82–84	33.63	5.09	26.16	4.83	17.19	69.72	55.92	86.91	19.78%	80.22%	64.34%
23	86–88	36.33	1.74	21.66	7.10	12.62	66.83	50.69	79.45	15.88%	84.12%	63.80%
24	90–92	38.03	6.12	21.28	5.35	21.56	70.77	65.71	92.34	23.35%	76.65%	71.16%
25	94–96	41.42	3.79	22.76	9.17	16.50	77.14	61.72	93.64	17.62%	82.38%	65.90%
26	98–100	41.33	15.80	23.21	6.60	15.06	86.93	72.18	101.99	14.76%	85.24%	70.77%
Mean		39.19	4.85	27.80	6.05	15.28	77.89	59.32	93.16	16.46%	83.54%	63.64%
Stdev		5.30	4.13	5.74	3.18	3.46	8.26	8.35	8.14	3.75%	3.75%	6.29%

Table A2. Sampling site M1-S1.

Sample Number	Depth (cm)	Ex-P	Concentrations (mg/kg)						TP	Percentage to TP (%)		
			Fe-P	Ca-P	De-P	OP	IP	BAP		OP	IP	BAP
1	0–2	30.24	3.83	36.16	3.03	6.12	73.26	40.19	79.38	7.72%	92.28%	50.99%
2	2–4	38.54	6.01	24.73	2.64	17.97	71.93	62.53	89.90	19.99%	80.01%	69.55%
3	6–8	38.70	3.85	24.33	3.85	16.47	70.73	59.01	87.20	18.88%	81.12%	67.68%
4	10–12	42.30	5.23	18.87	5.24	12.52	71.64	60.06	84.17	14.44%	85.56%	71.33%
5	14–16	41.64	2.33	21.37	4.18	6.90	69.52	50.87	76.42	9.02%	90.98%	66.57%
6	18–20	46.31	4.46	19.73	5.07	5.61	75.57	56.38	81.18	6.91%	93.09%	69.45%
7	22–24	40.33	3.86	19.80	4.17	6.91	68.16	51.11	75.07	9.21%	90.79%	68.08%
8	26–28	37.83	6.00	16.71	2.94	10.79	63.48	54.61	74.26	14.52%	85.48%	73.54%
9	30–32	36.21	5.03	13.50	4.12	5.06	58.85	46.29	63.91	7.91%	92.09%	72.43%
10	34–36	38.78	8.39	12.95	4.74	4.53	64.86	51.70	69.39	6.53%	93.47%	74.51%
11	38–40	39.51	6.28	14.82	3.84	3.41	64.45	49.20	67.86	5.03%	94.97%	72.50%
12	42–44	37.92	7.18	15.70	7.79	4.51	68.60	49.62	73.11	6.17%	93.83%	67.86%
13	46–48	38.86	5.97	17.54	5.06	7.28	67.43	52.11	74.70	9.74%	90.26%	69.75%
14	50–52	37.73	5.98	16.36	6.29	4.89	66.36	48.60	71.25	6.86%	93.14%	68.21%
15	54–56	41.95	4.42	16.83	3.21	8.77	66.40	55.13	75.17	11.66%	88.34%	73.35%
16	58–60	39.23	4.45	20.32	5.06	4.52	69.06	48.20	73.58	6.14%	93.86%	65.51%
17	62–64	40.45	7.45	14.71	4.42	5.80	67.03	53.69	72.82	7.96%	92.04%	73.73%
18	66–68	36.76	5.98	14.51	6.28	3.23	63.53	45.97	66.76	4.84%	95.16%	68.86%
19	70–72	37.88	7.18	17.82	5.05	12.94	67.92	58.00	80.86	16.00%	84.00%	71.72%
20	74–76	40.67	5.05	16.32	3.53	6.90	65.58	52.62	72.47	9.52%	90.48%	72.61%
21	78–80	31.35	6.23	12.29	10.47	4.70	60.35	42.28	65.04	7.22%	92.78%	65.01%
22	82–84	37.28	6.93	14.90	9.69	7.66	68.79	51.86	76.45	10.02%	89.98%	67.84%
23	86–88	36.34	9.68	22.86	6.00	5.79	74.88	51.81	80.67	7.18%	92.82%	64.22%
24	90–92	40.53	6.55	22.93	5.64	4.89	75.65	51.97	80.54	6.07%	93.93%	64.52%
25	94–96	38.75	6.61	18.55	8.75	6.88	72.66	52.24	79.54	8.65%	91.35%	65.68%
26	98–100	39.19	7.50	18.16	5.06	10.23	69.91	56.92	80.14	12.77%	87.23%	71.02%
Mean		38.66	5.86	18.57	5.24	7.51	68.33	52.04	75.84	9.65%	90.35%	68.71%
Stdev		3.16	1.61	4.96	2.01	3.83	4.34	5.17	6.47	4.11%	4.11%	4.75%

Table A3. Sampling site M2-L2.

Sample Number	Depth (cm)	Ex-P	Concentrations (mg/kg)						TP	Percentage to TP (%)		
			Fe-P	Ca-P	De-P	OP	IP	BAP		OP	IP	BAP
1	0–2	40.17	4.54	18.91	11.88	10.63	75.50	55.34	86.14	11.86%	88.14%	63.60%
2	2–4	33.89	4.12	18.06	7.86	13.30	63.94	51.32	77.24	17.22%	82.78%	66.44%
3	6–8	34.33	4.31	31.91	6.01	4.76	76.56	43.40	81.32	5.85%	94.15%	53.37%
4	10–12	34.60	5.84	28.02	12.80	7.47	81.25	47.91	88.72	8.41%	91.59%	53.92%
5	14–16	33.63	5.77	42.48	6.52	3.91	88.40	43.31	92.32	4.24%	95.76%	46.92%
6	18–20	32.74	8.13	43.53	7.37	9.31	91.76	50.18	101.07	9.21%	90.79%	49.64%
7	22–24	32.48	2.30	38.10	10.79	15.09	83.67	49.88	98.77	15.28%	84.72%	50.50%
8	26–28	36.28	3.82	56.27	14.94	14.03	111.31	54.13	125.34	11.19%	88.81%	43.19%
9	30–32	35.13	5.10	41.29	20.15	9.96	101.66	50.19	111.63	8.93%	91.07%	44.97%
10	34–36	34.24	2.31	22.68	16.22	15.71	75.45	52.27	91.16	17.23%	82.77%	57.33%
11	38–40	34.62	2.30	38.37	17.22	12.18	92.51	49.11	104.69	11.64%	88.36%	46.91%
12	42–44	31.67	2.49	30.86	19.52	14.97	84.53	49.12	99.50	15.04%	84.96%	49.37%
13	46–48	33.38	3.96	34.72	20.49	12.28	92.55	49.63	104.84	11.72%	88.28%	47.34%
14	50–52	33.35	3.33	28.48	14.69	8.11	79.85	44.79	87.96	9.22%	90.78%	50.92%
15	54–56	32.95	2.30	31.08	13.44	11.26	79.77	46.51	91.03	12.37%	87.63%	51.10%
16	58–60	33.94	2.33	34.21	11.19	5.84	81.67	42.11	87.51	6.68%	93.32%	48.12%
17	62–64	31.67	3.82	37.34	10.61	20.82	83.43	56.31	104.25	19.97%	80.03%	54.01%
18	66–68	35.23	5.98	42.54	16.04	17.53	99.79	58.75	117.32	14.94%	85.06%	50.08%
19	70–72	43.32	3.14	25.59	29.35	21.02	101.39	67.47	122.42	17.17%	82.83%	55.12%
20	74–76	35.57	3.28	22.50	31.57	9.15	92.92	48.00	102.07	8.96%	91.04%	47.03%
21	78–80	39.34	2.48	19.17	27.24	12.80	88.23	54.62	101.03	12.67%	87.33%	54.06%
22	82–84	41.75	2.79	16.37	16.91	16.78	77.83	61.32	94.61	17.73%	82.27%	64.82%
23	86–88	40.50	2.80	21.49	12.39	8.61	77.18	51.90	85.79	10.04%	89.96%	60.50%
24	90–92	46.23	3.65	18.70	24.91	6.50	93.49	56.38	99.99	6.50%	93.50%	56.38%
25	94–96	40.67	5.62	12.71	21.05	19.09	80.05	65.38	99.14	19.26%	80.74%	65.95%
26	98–100	42.04	3.33	15.51	4.95	25.14	65.83	70.51	90.97	27.64%	72.36%	77.51%
Mean		36.30	3.84	29.65	15.62	12.55	85.41	52.69	97.95	12.73%	87.27%	54.20%
Stdev		4.03	1.49	10.88	7.16	5.37	11.05	7.31	11.93	5.29%	5.29%	8.08%

Table A4. Sampling site M2-S2.

Sample Number	Depth (cm)	Ex-P	Concentrations (mg/kg)						TP	Percentage to TP (%)		
			Fe-P	Ca-P	De-P	OP	IP	BAP		OP	IP	BAP
1	0–2	31.71	1.32	6.76	14.59	5.86	52.81	37.33	58.67	9.82%	90.18%	63.49%
2	2–4	29.32	8.81	7.98	14.08	4.39	60.19	42.52	64.58	6.79%	93.21%	65.84%
3	6–8	28.26	4.30	9.47	13.01	12.41	55.05	44.97	67.45	18.39%	81.61%	66.66%
4	10–12	30.04	12.11	6.85	14.29	8.16	55.96	42.99	64.13	12.04%	87.96%	65.91%
5	14–16	30.22	0.50	9.94	1.89	8.10	42.56	38.82	50.65	15.98%	84.02%	76.64%
6	18–20	30.46	1.04	8.47	2.69	7.51	42.67	39.01	50.18	14.96%	85.04%	77.75%
7	22–24	32.40	6.00	12.05	15.35	12.96	65.79	51.36	78.75	16.46%	83.54%	65.22%
8	26–28	27.95	6.81	5.44	17.52	11.52	57.72	46.28	69.23	16.63%	83.37%	66.84%
9	30–32	32.01	3.54	7.13	4.37	8.35	47.04	43.90	55.39	15.08%	84.92%	79.24%
10	34–36	34.30	12.86	6.82	25.51	4.87	79.49	52.03	84.36	5.77%	94.23%	61.68%
11	38–40	32.49	5.46	7.67	12.08	5.30	57.71	43.26	63.01	8.41%	91.59%	68.65%
12	42–44	36.36	1.59	4.33	5.97	24.58	48.24	62.52	72.82	33.76%	66.24%	85.86%
13	46–48	36.73	3.54	6.58	15.71	12.71	62.56	52.98	75.27	16.89%	83.11%	70.38%
14	50–52	37.89	0.78	8.81	24.32	6.12	71.78	44.78	77.91	7.86%	92.14%	57.48%
15	54–56	36.45	0.49	7.63	17.24	6.04	61.81	42.98	67.85	8.90%	91.10%	63.35%
16	58–60	30.91	1.33	6.30	4.09	1.95	42.63	34.19	44.58	4.37%	95.63%	76.68%
17	62–64	31.13	1.31	2.95	14.72	13.68	50.12	46.13	63.80	21.44%	78.56%	72.30%
18	66–68	32.29	1.05	3.26	18.75	9.37	55.35	42.72	64.72	14.48%	85.52%	66.00%
19	70–72	29.13	4.31	4.58	16.04	5.96	54.07	39.41	60.03	9.93%	90.07%	65.65%
20	74–76	37.72	3.56	1.89	18.28	10.02	61.44	51.29	71.46	14.02%	85.98%	71.78%
21	78–80	31.59	5.45	6.55	24.16	6.28	67.76	43.32	74.03	8.48%	91.52%	58.51%
22	82–84	29.61	16.30	7.43	16.58	5.35	69.92	51.26	75.27	7.11%	92.89%	68.10%
23	86–88	41.82	1.61	17.42	5.49	6.68	66.33	50.11	73.01	9.15%	90.85%	68.63%
24	90–92	31.95	0.77	7.88	22.65	14.10	63.25	46.82	77.35	18.23%	81.77%	60.53%
25	94–96	37.94	2.72	5.21	26.29	11.63	72.16	52.29	83.79	13.88%	86.12%	62.40%
Mean		32.83	4.30	7.18	14.63	8.96	58.58	45.73	67.53	13.15%	86.85%	68.22%
Stddev		3.61	4.24	3.11	7.20	4.63	9.87	6.19	10.35	6.26%	6.26%	6.85%

References

- Henriques, M.; Granadeiro, J.P.; Piersma, T.; Leao, S.; Pontes, S.; Catry, T. Assessing the contribution of mangrove carbon and of other basal sources to intertidal flats adjacent to one of the largest West African mangrove forests. *Mar. Environ. Res.* **2021**, *169*, 105331. [\[CrossRef\]](#) [\[PubMed\]](#)
- Wang, G.; Singh, M.; Wang, J.; Xiao, L.; Guan, D. Effects of marine pollution, climate, and tidal range on biomass and sediment organic carbon in Chinese mangrove forests. *Catena* **2021**, *202*, 105270. [\[CrossRef\]](#)
- Zakaria, R.; Chen, G.; Chew, L.L.; Sofawi, A.B.; Moh, H.H.; Chen, S.; Teoh, H.W.; Adibah, S.Y.S.N. Carbon stock of disturbed and undisturbed mangrove ecosystems in Klang Straits, Malaysia. *J. Sea Res.* **2021**, *176*, 102113. [\[CrossRef\]](#)
- Bhandari, U.; Arulkumar, A.; Ganeshkumar, A.; Paramasivam, S.; Rajaram, R.; Miranda, J.M. Metal accumulation and biomineralisation of coastal and mangrove-associated molluscs of Palk Bay, Southeastern India. *Mar. Pollut. Bull.* **2021**, *167*, 112259. [\[CrossRef\]](#)
- Lewis, D.B.; Jimenez, K.L.; Abd-Elrahman, A.; Andreu, M.G.; Landry, S.M.; Northrop, R.J.; Campbell, C.; Flower, H.; Rains, M.C.; Richards, C.L. Carbon and nitrogen pools and mobile fractions in surface soils across a mangrove saltmarsh ecotone. *Sci. Total Environ.* **2021**, *798*, 149328. [\[CrossRef\]](#)
- Puthusseri, R.M.; Nair, H.P.; Johnny, T.K.; Bhat, S.G. Insights into the response of mangrove sediment microbiomes to heavy metal pollution: Ecological risk assessment and metagenomics perspectives. *J. Environ. Manag.* **2021**, *298*, 113492. [\[CrossRef\]](#)
- Pérez, A.; Machado, W.; Gutiérrez, D.; Saldarriaga, M.S.; Sanders, C.J. Shrimp farming influence on carbon and nutrient accumulation within Peruvian mangroves sediments. *Estuar. Coast. Shelf Sci.* **2020**, *243*, 106879. [\[CrossRef\]](#)
- Alongi, D.M. Mangrove forests: Resilience, protection from tsunamis, and responses to global climate change. *Estuar. Coast. Shelf Sci.* **2008**, *76*, 1–13. [\[CrossRef\]](#)
- Alam, M.I.; Ahsan, M.N.; Debrot, A.O.; Verdegem, M.C.J. Nutrients and anti-nutrients in leaf litter of four selected mangrove species from the Sundarbans, Bangladesh and their effect on shrimp (*Penaeus monodon*, Fabricius, 1798) post larvae. *Aquaculture* **2021**, *542*, 736865. [\[CrossRef\]](#)
- Liu, X.; Liu, H.; Chen, L.; Wang, X. Ecological interception effect of mangroves on microplastics. *J. Hazard Mater.* **2022**, *423*, 127231. [\[CrossRef\]](#)
- Pradit, S.; Noppradit, P.; Loh, P.-S.; Nitiratsuwan, T.; Le, T.P.Q.; Oeurng, C.; Mohamed, C.A.R.; Lee, C.W.; Lu, X.; Anshari, G.Z.; et al. The Occurrence of Microplastics in Sediment Cores from Two Mangrove Areas in Southern Thailand. *J. Mar. Sci. Eng.* **2022**, *10*, 418. [\[CrossRef\]](#)
- Vanegas, J.; Muñoz-García, A.; Pérez-Parra, K.A.; Figueroa-Galvis, I.; Mestanza, O.; Polanía, J. Effect of salinity on fungal diversity in the rhizosphere of the halophyte *Avicennia germinans* from a semi-arid mangrove. *Fungal Ecol.* **2019**, *42*, 100855. [\[CrossRef\]](#)
- Roy, A.K.D. Determinants of participation of mangrove-dependent communities in mangrove conservation practices. *Ocean. Coast. Manag.* **2014**, *98*, 70–78. [\[CrossRef\]](#)

14. Hyacinthe, C.; Van Cappellen, P. An authigenic iron phosphate phase in estuarine sediments: Composition, formation and chemical reactivity. *Mar. Chem.* **2004**, *91*, 227–251. [[CrossRef](#)]
15. Morales, M.I.; Masagca, J.T.; Araojo, A.E.; Vargas, S.R. Coastal and Mangrove Eco-Tourism in Catanduanes Island (Philippines): A Menace or a Bonus? In Proceedings of the International Conference on Latest Trends in Food, Biological & Ecological Sciences, Phuket, Thailand, 15–16 July 2014; pp. 15–16.
16. Mohammad, N.N.; Sarker, R.A.H.M.; Biswajit, N.; Eivin, R.; Ma, S.; Paul, K. Economic valuation of tourism of the Sundarban Mangroves, Bangladesh. *J. Ecol. Nat. Environ.* **2021**, *13*, 100–109. [[CrossRef](#)]
17. Asbridge, E.; Lucas, R.; Accad, A.; Dowling, R. Mangrove Response to Environmental Changes Predicted Under Varying Climates: Case Studies from Australia. *Curr. For. Rep.* **2015**, *1*, 178–194. [[CrossRef](#)]
18. Payo, A.; Mukhopadhyay, A.; Hazra, S.; Ghosh, T.; Ghosh, S.; Brown, S.; Nicholls, R.J.; Bricheno, L.; Wolf, J.; Kay, S.; et al. Projected changes in area of the Sundarban mangrove forest in Bangladesh due to SLR by 2100. *Clim Chang.* **2016**, *139*, 279–291. [[CrossRef](#)]
19. Aslan, A.; Rahman, A.F.; Robeson, S.M.; Iلمان, M. Land-use dynamics associated with mangrove deforestation for aquaculture and the subsequent abandonment of ponds. *Sci. Total Environ.* **2021**, *791*, 148320. [[CrossRef](#)]
20. Barbier, E.B. Economics: Account for depreciation of natural capital. *Nature* **2014**, *515*, 32–33. [[CrossRef](#)]
21. Andree, C.; Marie Anne Eurie, F.; Niels, T.; Isabel, G.A.; Arne, D.; Wout, V.E.; Lenin, R.F.; Jasmine, R.; Liesbeth, J.; Pieter, S.; et al. From field to plate: Agricultural pesticide presence in the guayas estuary (Ecuador) and commercial mangrove crabs. *Environ. Pollut.* **2021**, *289*, 117955. [[CrossRef](#)]
22. Banerjee, S.; Ghosh, S.; Singh, K.; Ghodke, M.; Sudarshan, M. Detection of metals and associated bacteria from Mumbai mangroves and their impact analysis. *Reg. Stud. Mar. Sci.* **2021**, *48*, 102007. [[CrossRef](#)]
23. Kesavan, S.; Xavier, K.A.M.; Deshmukhe, G.; Jaiswar, A.K.; Bhusan, S.; Shukla, S.P. Anthropogenic pressure on mangrove ecosystems: Quantification and source identification of surficial and trapped debris. *Sci. Total Environ.* **2021**, *794*, 148677. [[CrossRef](#)] [[PubMed](#)]
24. Rodríguez-Rodríguez, J.A.; Mancera-Pineda, J.E.; Tavera, H. Mangrove restoration in Colombia: Trends and lessons learned. *For. Ecol. Manag.* **2021**, *496*, 119414. [[CrossRef](#)]
25. Wayan Eka Dharmawan, I. Mangrove health index distribution on the restored post-tsunami mangrove area in Biak Island, Indonesia. *IOP Conf. Ser. Earth Environ. Sci.* **2021**, *860*, 012007. [[CrossRef](#)]
26. Hanggara, B.B.; Murdiyarso, D.; Ginting, Y.R.S.; Widha, Y.L.; Panjaitan, G.Y.; Lubis, A.A. Effects of diverse mangrove management practices on forest structure, carbon dynamics and sedimentation in North Sumatra, Indonesia. *Estuar. Coast. Shelf Sci.* **2021**, *259*, 107467. [[CrossRef](#)]
27. Tachas, J.N.; Raoult, V.; Morris, R.L.; Swearer, S.E.; Gaston, T.F.; Strain, E.M.A. Eco-engineered mangroves provide complex but functionally divergent niches for estuarine species compared to natural mangroves. *Ecol. Eng.* **2021**, *170*, 106355. [[CrossRef](#)]
28. Maza, M.; Lara, J.L.; Losada, I.J. Predicting the evolution of coastal protection service with mangrove forest age. *Coast. Eng.* **2021**, *168*, 103922. [[CrossRef](#)]
29. Agaton, C.B.; Collera, A.A. Now or later? Optimal timing of mangrove rehabilitation under climate change uncertainty. *For. Ecol. Manag.* **2022**, *503*, 119739. [[CrossRef](#)]
30. Xia, X.; Wu, Q.; Zhu, B.; Zhao, P.; Zhang, S.; Yang, L. Analyzing the contribution of climate change to long-term variations in sediment nitrogen sources for reservoirs/lakes. *Sci. Total Environ.* **2015**, *523*, 64–73. [[CrossRef](#)]
31. Zhang, H.; Huo, S.; Yeager, K.M.; He, Z.; Xi, B.; Li, X.; Ma, C.; Wu, F. Phytoplankton response to climate changes and anthropogenic activities recorded by sedimentary pigments in a shallow eutrophied lake. *Sci. Total Environ.* **2019**, *647*, 1398–1409. [[CrossRef](#)]
32. Guignard, M.S.; Leitch, A.R.; Acquisti, C.; Eizaguirre, C.; Elser, J.J.; Hessen, D.O.; Jeyasingh, P.D.; Neiman, M.; Richardson, A.E.; Soltis, P.S.; et al. Impacts of Nitrogen and Phosphorus: From Genomes to Natural Ecosystems and Agriculture. *Front. Ecol. Evol.* **2017**, *5*, 70. [[CrossRef](#)]
33. Johnson, A.C.; Acreman, M.C.; Dunbar, M.J.; Feist, S.W.; Giacomello, A.M.; Gozlan, R.E.; Hinsley, S.A.; Ibbotson, A.T.; Jarvie, H.P.; Jones, J.I.; et al. The British river of the future: How climate change and human activity might affect two contrasting river ecosystems in England. *Sci. Total Environ.* **2009**, *407*, 4787–4798. [[CrossRef](#)] [[PubMed](#)]
34. Coelho, J.P.; Flindt, M.R.; Jensen, H.S.; Lillebø, A.I.; Pardal, M.A. Phosphorus speciation and availability in intertidal sediments of a temperate estuary: Relation to eutrophication and annual P-fluxes. *Estuar. Coast. Shelf Sci.* **2004**, *61*, 583–590. [[CrossRef](#)]
35. Hiriart-Baer, V.P.; Milne, J.E.; Marvin, C.H. Temporal trends in phosphorus and lacustrine productivity in Lake Simcoe inferred from lake sediment. *J. Great Lakes Res.* **2011**, *37*, 764–771. [[CrossRef](#)]
36. Bastami, K.D.; Neyestani, M.R.; Raeisi, H.; Shafeian, E.; Baniamam, M.; Shirzadi, A.; Esmailzadeh, M.; Mozaffari, S.; Shahrokhi, B. Bioavailability and geochemical speciation of phosphorus in surface sediments of the Southern Caspian Sea. *Mar. Pollut. Bull.* **2018**, *126*, 51–57. [[CrossRef](#)]
37. Cavalcante, H.; Araujo, F.; Noyma, N.P.; Becker, V. Phosphorus fractionation in sediments of tropical semiarid reservoirs. *Sci. Total Environ.* **2018**, *619*, 1022–1029. [[CrossRef](#)]
38. Cong, M.; Jiang, T.; Qi, Y.-z.; Dong, H.-p.; Teng, D.-q.; Lu, S.-h. Phosphorus forms and distribution in Zhejiang coastal sediment in the East China Sea. *Int. J. Sediment Res.* **2014**, *29*, 278–284. [[CrossRef](#)]
39. Kang, X.; Song, J.; Yuan, H.; Shi, X.; Yang, W.; Li, X.; Li, N.; Duan, L. Phosphorus speciation and its bioavailability in sediments of the Jiaozhou Bay. *Estuar. Coast. Shelf Sci.* **2017**, *188*, 127–136. [[CrossRef](#)]

40. Loh, P.S.; Molot, L.A.; Nowak, E.; Nürnberg, G.K.; Watson, S.B.; Ginn, B. Evaluating relationships between sediment chemistry and anoxic phosphorus and iron release across three different water bodies. *Inland Waters* **2013**, *3*, 105–118. [[CrossRef](#)]
41. Soliman, N.F.; El Zokm, G.M.; Okbah, M.A. Evaluation of phosphorus bioavailability in El Mex Bay and Lake Mariut sediments. *Int. J. Sediment Res.* **2017**, *32*, 432–441. [[CrossRef](#)]
42. Barcellos, D.; Queiroz, H.M.; Nobrega, G.N.; de Oliveira Filho, R.L.; Santaella, S.T.; Otero, X.L.; Ferreira, T.O. Phosphorus enriched effluents increase eutrophication risks for mangrove systems in northeastern Brazil. *Mar. Pollut. Bull.* **2019**, *142*, 58–63. [[CrossRef](#)] [[PubMed](#)]
43. Jiang, S.; Lu, H.; Liu, J.; Lin, Y.; Dai, M.; Yan, C. Influence of seasonal variation and anthropogenic activity on phosphorus cycling and retention in mangrove sediments: A case study in China. *Estuar. Coast. Shelf Sci.* **2018**, *202*, 134–144. [[CrossRef](#)]
44. Weng, C.H.; Wang, D.G.; Han, F.J.; Shen, G.; Tan, Y.H.; Lv, D.A.; Weerasinghe, R. Study on the Driving Mechanism of Ecosystem Service Value on Ximen Island Based on STIRPAT Model. *E3S Web Conf.* **2018**, *53*, 03036. [[CrossRef](#)]
45. Zhang, Z.; Hu, G.; Liang, S. Distribution, protection and ecological value of mangroves in China. *Bull. Biol.* **2006**, *64*, 9–11. (In Chinese) [[CrossRef](#)]
46. Du, P.; Liu, J.; Zeng, J.; Chen, Q.; Zhu, X.; Gao, Y. Bacteria distribution and environmental characteristics in the sediment of Ximen Island mangrove. *Mar. Environ. Sci.* **2014**, *33*, 763–771. (In Chinese) [[CrossRef](#)]
47. Wang, A.; Chen, J.; Jing, C.; Ye, G.; Wu, J.; Huang, Z.; Zhou, C. Monitoring the Invasion of *Spartina alterniflora* from 1993 to 2014 with Landsat TM and SPOT 6 Satellite Data in Yueqing Bay, China. *PLoS ONE* **2015**, *10*, e0135538. [[CrossRef](#)]
48. Zheng, J.; Wang, J.; Chen, Q.; Xu, J.; Li, X.; Lu, X.; Lei, H.; Zheng, S. Preliminary report on north-ward introduction experiment of several mangrove plants along the southern coast of Zhejiang Province. *J. Southwest For. Univ.* **2010**, *30*, 11–17. (In Chinese)
49. Li, J.; Xu, H. Introduction and Afforestation Technique of *Kandelia candel* to the North. *J. Zhejiang For. Sci. Technol.* **2001**, *23*, 6–8. (In Chinese)
50. Zhu, H.; Guo, Y.; Wu, C.; Zhang, L. Study on meiofauna abundance in mangrove of Ximen Island, Zhejiang province. *J. Jimei Univ. Nat. Sci.* **2020**, *25*, 241–247. (In Chinese) [[CrossRef](#)]
51. Liao, Y.; Shou, L.; Tang, Y.; Zeng, J.; Chen, Q.; Yan, X. Effects of non-indigenous plants on food sources of intertidal macrobenthos in Yueqing Bay, China: Combining stable isotope and fatty acid analyses. *Estuar. Coast. Shelf Sci.* **2020**, *241*, 106801. [[CrossRef](#)]
52. Wang, Q.; Song, L.; Agusti, S.; Duarte, C.; Christakos, G.; Wu, J. Changes of the Macrobenthos Community with Non-native Mangrove Rehabilitation (*Kandelia obovata*) and Salt Marsh Invasion (*Spartina alterniflora*) in Ximen Island, Zhejiang, China. *Ocean Sci. J.* **2021**, *56*, 395–405. [[CrossRef](#)]
53. Chen, Q.; Yang, S.; Wang, J.; Liu, X.; Deng, R. Development history and discussion of mangrove forest in Zhejiang Province. *J. Zhejiang Agric. Sci.* **2019**, *60*, 1177–1181. (In Chinese) [[CrossRef](#)]
54. Zhou, Z.; Xu, G.; Chen, Y.; Lin, Z. Ximen Island: “Guardian” of the northernmost mangroves area. *Map* **2020**, *3*, 56–69. (In Chinese)
55. Ruttenberg, K.C. Development of a sequential extraction method for different forms of phosphorus in marine sediments. *Limnol. Oceanogr.* **1992**, *37*, 1460–1482. [[CrossRef](#)]
56. Ruttenberg, K.C.; Berner, R.A. Authigenic apatite formation and burial in sediments from non-upwelling, continental margin environments. *Geochim. Cosmochim. Acta* **1993**, *57*, 991–1007. [[CrossRef](#)]
57. Andrieux-Loyer, F.; Aminot, A. Phosphorus Forms Related to Sediment Grain Size and Geochemical Characteristics in French Coastal Areas. *Estuar. Coast. Shelf Sci.* **2001**, *52*, 617–629. [[CrossRef](#)]
58. Kaiserli, A.; Voutsas, D.; Samara, C. Phosphorus fractionation in lake sediments—Lakes Volvi and Koronia, N. Greece. *Chemosphere* **2002**, *46*, 1147–1155. [[CrossRef](#)]
59. Lake, B.A.; Coolidge, K.M.; Norton, S.A.; Amirbahman, A. Factors contributing to the internal loading of phosphorus from anoxic sediments in six Maine, USA, lakes. *Sci. Total Environ.* **2007**, *373*, 534–541. [[CrossRef](#)]
60. Norton, S.A.; Coolidge, K.; Amirbahman, A.; Bouchard, R.; Kopacek, J.; Reinhardt, R. Speciation of Al, Fe, and P in recent sediment from three lakes in Maine, USA. *Sci. Total Environ.* **2008**, *404*, 276–283. [[CrossRef](#)]
61. Zhuang, W.; Gao, X.; Zhang, Y.; Xing, Q.; Tosi, L.; Qin, S. Geochemical characteristics of phosphorus in surface sediments of two major Chinese mariculture areas: The Laizhou Bay and the coastal waters of the Zhangzi Island. *Mar. Pollut. Bull.* **2014**, *83*, 343–351. [[CrossRef](#)]
62. Andrieux, F.; Aminot, A. A two-year survey of phosphorus speciation in the sediments of the Bay of Seine (France). *Cont. Shelf Res.* **1997**, *17*, 1229–1245. [[CrossRef](#)]
63. Yang, Y.; Gao, B.; Hao, H.; Zhou, H.; Lu, J. Nitrogen and phosphorus in sediments in China: A national-scale assessment and review. *Sci. Total Environ.* **2017**, *576*, 840–849. [[CrossRef](#)] [[PubMed](#)]
64. Sekula-Wood, E.; Benitez-Nelson, C.R.; Bennett, M.A.; Thunell, R. Magnitude and composition of sinking particulate phosphorus fluxes in Santa Barbara Basin, California. *Glob. Biogeochem. Cycles* **2012**, *26*. [[CrossRef](#)]
65. Yang, B.; Liu, S.-M.; Wu, Y.; Zhang, J. Phosphorus speciation and availability in sediments off the eastern coast of Hainan Island, South China Sea. *Cont. Shelf Res.* **2016**, *118*, 111–127. [[CrossRef](#)]
66. Meng, J.; Yao, P.; Yu, Z.; Bianchi, T.S.; Zhao, B.; Pan, H.; Li, D. Speciation, bioavailability and preservation of phosphorus in surface sediments of the Changjiang Estuary and adjacent East China Sea inner shelf. *Estuar. Coast. Shelf Sci.* **2014**, *144*, 27–38. [[CrossRef](#)]
67. Ni, J.; Lin, P.; Zhen, Y.; Yao, X.; Guo, L. Distribution, source and chemical speciation of phosphorus in surface sediments of the central Pacific Ocean. *Deep Sea Res. Part I* **2015**, *105*, 74–82. [[CrossRef](#)]

68. Nobrega, G.N.; Otero, X.L.; Macias, F.; Ferreira, T.O. Phosphorus geochemistry in a Brazilian semiarid mangrove soil affected by shrimp farm effluents. *Environ. Monit. Assess* **2014**, *186*, 5749–5762. [[CrossRef](#)]
69. Ji, X.; Zhang, Y.; Zhu, D. Study on marine environment and recent coastal evolution of Yueqing Bay, Zhejiang province, China. *Mar. Sci. Bull.* **2006**, *25*, 44–53. (In Chinese) [[CrossRef](#)]
70. Hu, J.; Loh, P.S.; Pradit, S.; Le, T.P.Q.; Oeurng, C.; Mohamed, C.A.R.; Lee, C.W.; Lu, X.; Anshari, G.Z.; Kandasamy, S.; et al. Assessing the Effect of Age and Geomorphic Setting on Organic Carbon Accumulation in High-Latitude Human-Planted Mangroves. *Forests* **2022**, *13*, 105. [[CrossRef](#)]
71. Bala Krishna Prasad, M.; Ramanathan, A.L. Characterization of phosphorus fractions in the sediments of a tropical intertidal mangrove ecosystem. *Wetl. Ecol. Manag.* **2009**, *18*, 165–175. [[CrossRef](#)]
72. Le, Y.; Hu, M.; Lai, X.; Wang, Y.; Xiao, L.; Wang, S.; Li, T.; Zhou, S. Changes of phosphorus speciation and enzyme activities in sediments of the Quanzhou Bay estuarine wetland under different vegetation restoration patterns. *Acta Sci. Circumstantiae* **2022**, *4*, 1–9. (In Chinese) [[CrossRef](#)]
73. Xiong, Y.; Liao, B.; Proffitt, E.; Guan, W.; Sun, Y.; Wang, F.; Liu, X. Soil carbon storage in mangroves is primarily controlled by soil properties: A study at Dongzhai Bay, China. *Sci. Total Environ.* **2018**, *619*, 1226–1235. [[CrossRef](#)] [[PubMed](#)]
74. Feng, J.; Zhou, J.; Wang, L.; Cui, X.; Ning, C.; Wu, H.; Zhu, X.; Lin, G. Effects of short-term invasion of *Spartina alterniflora* and the subsequent restoration of native mangroves on the soil organic carbon, nitrogen and phosphorus stock. *Chemosphere* **2017**, *184*, 774–783. [[CrossRef](#)] [[PubMed](#)]
75. Sonzogni, W.C.; Chapra, S.C.; Armstrong, D.E.; Logan, T.J. Bioavailability of Phosphorus Inputs to Lakes. *J. Environ. Qual.* **1982**, *11*, 555–563. [[CrossRef](#)]
76. Zhang, J.-E.; Liu, J.-L.; Ouyang, Y.; Liao, B.-W.; Zhao, B.-L. Removal of nutrients and heavy metals from wastewater with mangrove *Sonneratia apetala* Buch-Ham. *Ecol. Eng.* **2010**, *36*, 807–812. [[CrossRef](#)]
77. Chen, H.; Liao, B.; Liu, B.; Peng, C.; Zhang, Y.; Guan, W.; Zhu, Q.; Yang, G. Eradicating invasive *Spartina alterniflora* with alien *Sonneratia apetala* and its implications for invasion controls. *Ecol. Eng.* **2014**, *73*, 367–372. [[CrossRef](#)]
78. Ahlgren, J.; Tranvik, L.; Gogoll, A.; Waldebäck, M.; Markides, K.; Rydin, E. Sediment Depth Attenuation of Biogenic Phosphorus Compounds Measured by ³¹P NMR. *Environ. Sci. Technol.* **2005**, *39*, 867–872. [[CrossRef](#)]
79. Borges, A.; Sanders, C.; Santos, H.; Araripe, D.; Machado, W.; Patchineelam, S. Accumulation of paralytic shellfish toxins in digestive gland of *Octopus vulgaris* during bloom events including the dinoflagellate *Gymnodinium catenatum*. *Mar. Pollut. Bull.* **2009**, *58*, 1747–1750. [[CrossRef](#)]
80. Feng, J.; Cui, X.; Zhou, J.; Wang, L.; Zhu, X.; Lin, G. Effects of exotic and native mangrove forests plantation on soil organic carbon, nitrogen, and phosphorus contents and pools in Leizhou, China. *Catena* **2019**, *180*, 1–7. [[CrossRef](#)]